T. & A. M. REPORT NO. 342

NASA CR-72949

CREEP DEFORMATION BEHAVIOR OF METALS UNDER REPEATED STRESS REVERSALS

Final Report

by

Masaki Kitagawa and JoDean Morrow

Sponsored by

National Aeronautics and Space Administration
Lewis Research Center
Research Grant NGR-14-005-025

Department of Theoretical and Applied Mechanics
University of Illinois
Urbana, Illinois

June 1971

FOREWORD

This investigation was conducted in the H. F. Moore Fracture Research Laboratory of the Department of Theoretical and Applied Mechanics at the University of Illinois, Urbana, Illinois. Financial support was provided by the National Aeronautics and Space Administration under Research Grant NGR-14-005-025, and by the Research Borad of the University of Illinois, Urbana, Illinois.

The following individuals: Dr. G. R. Halford, Dr. P. A. Lilienthal, Mr. C. E. Jaske, and Mr. Masaki Kitagawa, participated in this research as a part of their graduate theses research. The following three senior students: L. B. Freund, Howard Rosenmayer, and R. A. Testin, performed research under this program as a part of their senior projects.

Papers produced during this study are included in the list of references at the end of this report and are referred to whenever the subject appears in the text.

ABSTRACT

Reversed creep tests on chemical lead, 1100-F aluminum and OFHC copper were conducted and creep deformation behavior under repeated stress reversals was studied. Metallographic observations were also made to determine the nature of the structural alteration accompanying reversed creep deformation.

It is shown that the creep deformation resistance of a variety of metals is reduced by repeated reversed deformation at temperatures above $0.4T_m$, where T_m is the absolute melting temperature of each metal. The reduction of creep deformation resistance due to stress reversals is most prominent at approximately $0.5T_m$, and it is of a persistent nature. Metallographic studies show that the observed acceleration of creep at high temperatures is in part due to the enhancement of grain boundary sliding as a result of gradual grain boundary migration toward planes of maximum shear stress during reversed creep deformation.

INTRODUCTION

Creep deformation behavior of metals subjected to nonsteady stressing has been reviewed by several authors (1-5). The experiments cited in these reviews include creep tests under intermittent, cyclic and step loading. Data are also cited on the effect of over-stressing and rapid loading and on dynamic creep tests in which metals are subjected to alternating stress superimposed on a constant mean stress. In spite of the variety of loading conditions employed, in most of these tests the stress was limited to tension so that the effect of reversing the stress was ignored. Even in those rare cases where the stress is reversed, only the accumulation of tensile deformation is measured and no detailed study has been made of creep deformation during reversed stressing.

An understanding of the influence of stress reversals on creep deformation resistance is of fundamental and practical importance. It will be seen that reversed stressing may cause an unexpected large decrease in the creep deformation resistance of a metal. Thus, existing methods of designing on the basis of static creep data and theory may be unsafe whenever the service stresses and/or temperatures are cyclic in nature.

Only a few studies have been made on the creep deformation of metals under stress reversals. These are summarized in Table 1. Andrade and Jolliffe (6) appear to be the first to have examined the effect of stress reversals on creep deformation behavior. Although they applied only one or two stress reversals, the results indicate that unusual effects are caused by stress reversals which are sometimes deleterious to creep deformation resistance. Later, Morrow and Halford (7) studied the effect more systematically using reversed torsional tests on lead at room temperature. They applied about 100 reversals and observed a continuous large acceleration of creep due to stress reversals. The observed effects were much larger than can be achieved by simply cycling the stress in one direction. This remarkable acceleration of reversed creep could not be readily explained on the bases of usual unidirectional creep results and existing theory.

The present investigation was aimed at clarifying the details of the phenomenological nature of creep deformation under repeated stress reversals. Associated structural changes were also examined in order to find the causes of the observed degradation of creep deformation resistance during reversed creep at high temperatures.

CREEP DEFORMATION BEHAVIOR OF METALS UNDER REPEATED STRESS REVERSALS

Reversed Creep Experiments

Tests were conducted on tubular specimens in torsion under the control conditions illustrated in Fig. 1. The apparatus and automatic control system is described in Appendix A. In each test the shear stress is maintained constant until a preset upper strain limit is reached. The stress is then reversed. When the total strain reaches the lower strain limit*, the stress is reversed again and maintained constant until the upper strain limit is again reached. Reversing was continued for about 60 to 70 reversals. A change in the creep deformation resistance of the metal will alter the period of time between reversals as shown in Fig. 1(b).

To represent the creep deformation resistance during one reversal an "average creep rate" was calculated by dividing the creep strain by the period of one reversal as defined in Fig. 1. Note that the measurement of a minimum creep rate is ambiguous in this type of test because steady state creep conditions are not necessarily reached.

Tests were conducted on 1100-F aluminum (99% purity) and chemical lead (99.9%). A limited number of tests were also performed on OFHC copper. Specimens were annealed under the conditions listed in Table 2 before testing.

Effect of Temperature on the Changes in Creep Deformation Resistance

Typical changes in the average creep rate from cycle to cycle are shown in Fig. 2. The results indicate that cyclic deformation may cause an increase or a decrease in creep deformation resistance depending on the test temperature. In order to examine the temperature dependence, ratios of the average creep rates before, $\bar{\dot{\gamma}}_o$, and after cycling**, $\bar{\dot{\gamma}}_r$, are plotted in Fig. 3 as a function of homologous temperature***.

---

* The lower strain limit was always set at zero except in the early part of the study (prior to 1965) when the strain was completely reversed (7).

** For convenience, the creep rate after about 60 stress reversals is taken as a representative creep rate after cycling. This may be justified because the creep rate change from one cycle to the next is much smaller after about 50 reversals than during the first several reversals.

***Homologous temperature is the temperature represented by the ratio of the absolute test temperature to the absolute melting temperature, T_m, of each metal.

The figure includes data on 1100-F aluminum (8), chemical lead (7, 9), magnesium (10), 20%Cr/25%Ni/Nb steel (11) and Inconel (12). For this variety of metals, homologous temperature appears to serve as an index for estimating whether acceleration or deceleration of creep will occur.

At temperatures less than $0.4\,T_m$, creep deformation resistance increases with the number of stress reversals. This deceleration of creep is similar to the cyclic hardening which is often found during fatigue tests of annealed metals at low homologous temperatures. At high temperatures, however, the average creep rate may increase as much as a factor of 10-20 times compared to uncycled specimens. Around $0.5\,T_m$, the acceleration of creep appears to be most pronounced (13).

Persistent Nature of Reversed Creep Acceleration

Freund (14) subjected several lead specimens to a constant stress after reversed creep testing until a steady creep rate was approached. Typical static creep curves before and after cycling are compared in Fig. 4. Note that the creep rate of the cycled specimen does not decrease to the steady creep rate of the uncycled specimen. Thus the acceleration of reversed creep is not of a transitory nature in the sense that the static creep resistance of the metal is permanently reduced even in the steady state creep region.

To further examine the persistent nature of reversed creep acceleration, cycled specimens were allowed to rest at zero stress at the test temperature. Sample results are shown in Fig. 5 for OFHC copper. In the case of aluminum and OFHC copper, the rest period appears to improve the creep deformation resistance slightly. The creep rate before resting is quickly reached in only a few cycles after resuming the stress reversing.

In terms of the microstructural alterations, the above observations imply that some persistent detrimental structural changes are caused by reversed cyclic deformation at high homologous temperatures and that the resultant structure cannot be restored by overstraining nor by rest periods around the test temperature.

Stress Dependence of Creep Rate

In Fig. 6 the stress dependence of the creep rate for cycled specimens is compared with that of uncycled specimens. A straight line relationship between stress and creep rate on the log-log coordinates means that a power function may be used to relate the variables in the range of observed creep rates. In the case of aluminum,

the stress dependence exponent is seen to be about the same for the creep rate before and after cycling. This exponent (about twelve) is approximately the same as that of tensile steady creep rate reported by Servi and Grant (15) for aluminum at $0.57\,T_m$, as shown in Fig. 6.

In the case of lead, the exponents for both the average creep rate and steady creep rate of cycled specimens appear to be nearly the same as for the aluminum, though it is much higher than for the steady creep rate of uncycled lead specimens. This indicates that the ratio of creep rates in Fig. 3 depends on the stress level for chemical lead but not for the 1100-F aluminum.

The observed change in the stress dependence exponent of lead as well as the above mentioned cyclic change in creep deformation resistance show that unidirectional static creep results are not applicable for the evaluation of the time dependent deformation of metals when subjected to stress reversals.

Parametric Representation of Reversed Creep

It has been shown that the reversed creep behavior of a metal is not reflected by static creep data. However, the creep strain rate of metals after reversed cycling may be approximated by a function of the homologous test temperature and the cyclic stress and strain level. As in the case of static creep, it may also be possible to characterize the reversed creep resistance using a parametric form of these variables.

Jaske (8) and Gain and Sinclair (16) have analyzed existing reversed creep data using time-temperature and stress-strain parameters. The utility of such a representation is that one can estimate the reversed creep behavior outside the range of temperature and stress covered in testing and for other metals for which there is not yet any reversed creep test data.

METALLOGRAPHIC STUDIES

Grain boundary migration was observed and grain boundary sliding was measured for lead during reversed creep. To measure grain boundary sliding, two sets of scratches were scribed on the surface of several lead specimens: one in the direction parallel to the torsional axis and the other perpendicular to it. Shear strain due to grain boundary sliding, γ_{gb}, was calculated by the following equation* (17):

$$\gamma_{gb} = \frac{U_1}{d_2} + \frac{U_2}{d_1}$$

where U_1 and U_2 are offsets of scratches across the grain boundaries and d_1 and d_2 are grain sizes. Subscripts indicate the direction of measurements.

Grain Boundary Migration during Reversed Creep

Virtually all the grain boundaries were observed to migrate toward the maximum shear planes during reversed creep of lead at room temperature. Figure 7 shows typical traces of the observed grain boundary migration. Cross sectional views of cycled specimens, shown in Fig. 8, illustrate that the resultant grains have an orthorhombic shape throughout the thickness of the specimen and that their boundaries are parallel or perpendicular to the maximum shear planes. For all the tests performed, the resultant orthorhombic grain size was larger than the initial grain size. Testin (19) has shown that the relation between stress and orthorhombic grain size of lead can be approximated by a linear function: $\tau_a = 55 + 2.25d^{-1}$, where d is grain size in inches and τ_a is applied shear stress in psi (Fig. 9).

When tubular specimens of lead were subjected to repeated axial reversed loading (axial fatigue), grain boundaries observed at the surface were found to migrate so that they were inclined at 45 degrees from the specimen axis. Surface layers of a specimen were removed chemically after 400 reversals under $\Delta\epsilon = 0.005$ applied at about two cycles per minute. It was found that the rectangular network of grain boundaries had been formed throughout the thickness of the tube. Similar grain structure has been reported in other metals (20-26) after fatigue tests at high temperatures.

---

*In axial creep studies, several equations for grain boundary sliding strain have been proposed. This is because the use of the definition of axial strain requires difficult and impractical measurements (18). For shear strain, however, the quantities in the above equation are directly measurable.

Enhancement of Grain Boundary Sliding

Gifkins et al. (27) have shown that the amount of grain boundary sliding, U_{gb}, in polycrystalline metals can be approximated by a power function of the resolved shear stress on each grain boundary τ_{rss}; that is $U_{gb} = A \tau_{rss}^{m}$.

In view of this observation, it is seen that the reorientation of grain boundaries from random directions into the maximum shear planes increases the sliding on each grain boundary. In Appendix B the expected increase in grain boundary sliding is calculated using this approximation. For example, when the exponent, m, is five, the reorientation of all the boundaries into the maximum shear planes could increase the average of grain boundary sliding by a factor of about eight.

Opposing the enhancement of grain boundary sliding may be the effect of an increase in grain size during reversed creep. Several investigations (28, 29) of unidirectional static creep indicate that an increase in grain size tends to decrease the ratio of γ_{gb} to over-all creep strain, γ_t. However, the effect appears to be small (28). For example, results on a lead-thallium alloy (29) would indicate that only a few per cent variation in the ratio, $\alpha = \gamma_{gb}/\gamma_t$, for the variation of grain size encountered in this investigation of lead. The observed ratios, α, in the uncycled specimens and in the cycled specimens are compared in Fig. 10, illustrating that the formation of the orthorhombic grain structure substantially increases the contribution of grain boundary sliding to over-all creep strain even though the grain size is increased by a factor of approximately two.

Since at high temperatures the grain boundaries have less deformation resistance than the grain, the enhancement of grain boundary sliding due to the formation of the orthorhombic grain structure is an important factor which causes a reduced creep deformation resistance (i.e. an acceleration of creep). The effect of reorientation of grain boundaries on the acceleration of creep is quantitatively evaluated in Appendix B. The results indicate that the effect will be larger the larger the stress dependence exponent, m, and the larger the strain ratio, α.

Relation between Changes in Creep Rate and Grain Structure

The cause for the observed acceleration of creep proposed above is substantiated by the following qualitative relations between the alterations of creep resistance and grain structure during reversed creep.

During the early stages of a high temperature reversed creep test, the increase in average creep rate is accompanied by a rapid formation of a rectangular network of grain boundaries. This is seen for the case of lead by comparing Figs. 2b and 11. As reversed stressing is continued, there is less increase in the average creep rate and only minor further development of the rectangular network.

At low homologous temperatures, where deceleration of creep is a general tendency, the orthorhombic structure may not be formed since the grain boundary migration is unlikely at low homologous temperatures.

The orthorhombic grain structure is believed to be quite stable. It was observed that the general view of the rectangular boundary network of lead had not changed at room temperature even several months after testing. In fact, Rosenmayer (30) found that temperatures above 150 C are required to recrystallize the orthorhombic grain structure. Furthermore, this structure cannot be easily eliminated by continuing unidirectional plastic strain. The stability of this structure coincides with the persistent nature of the reduced creep deformation resistance.

Reversed Creep Behavior of Impure Metals

The literature summarized in Table 3 confirms that the formation of an orthorhombic grain structure by means of gradual grain boundary migration is common in high-purity FCC metals during cyclic deformation at high temperatures. For those metals the formation of the orthorhombic grain structure would play an important role in the acceleration of creep. It is expected that the prevention of grain boundary migration would retard the acceleration of creep.

On the other hand, the acceleration of creep has been observed not only for pure metals but also for impure metals in which the formation of an orthorhombic grain structure is unlikely. In fact, reversed creep experiments on 1100-F aluminum and Inconel (12) show an acceleration of creep at high temperatures although the orthorhombic grain structure was not formed. This implies that there are some additional structural changes which cause the degradation of creep deformation resistance during repeated reversed loading at high temperatures.

SUMMARY

This investigation indicates that present methods of evaluating the creep deformation resistance of metals at high homologous temperatures may be in serious error if stresses are reversed. It is shown that the creep deformation resistance of a variety of metals is reduced by cyclic deformation at temperatures above $0.4T_m$. This degradation of creep deformation resistance is of a persistent nature.

From metallographic studies a mechanism for the cause of acceleration of creep is proposed for pure metals. Reversed stressing at high temperatures causes grain boundaries to migrate toward the maximum shear planes forming an orthorhombic grain structure. The formation of this orthorhombic grain structure increases the contribution of grain boundary sliding strain to over-all creep strain thereby reducing the creep deformation resistance of the metal. Retardation of grain boundary migration so that the orthorhombic structure has difficulty forming will reduce the acceleration of creep due to stress reversal. Yet a significant acceleration of creep may still occur, presumably due to additional factors not yet understood.

LIST OF REFERENCES

Note: References marked by an asterisk (*) are work performed as a part of this program.

1. S. S. Manson, "Creep under Nonsteady Temperatures and Stresses," Mechanical Behavior of Materials at Elevated Temperatures, J. E. Dorn, Editor, McGraw-Hill Book Co. Inc., New York, 1961, pp. 419-476.

2. A. H. Meleka, "Combined Creep and Fatigue Properties," Metallurgical Reviews, Vol. 7, No. 25, 1962, pp. 43-93.

3. Masateru Ohnami, "Creep under Nonsteady Stresses and Temperatures," Mechanical Behavior of Metals at Elevated Temperatures, Shuji Taira, Editor, Yokendo, Tokyo, Japan, 1968, pp. 210-240 (in Japanese).

4. Ryoichi Koterazawa, "Dynamic Creep and Fatigue at Elevated Temperatures," Mechanical Behavior of Metals at Elevated Temperatures, Shuji Taira, Editor, Yokendo, Tokyo, Japan, 1968, pp. 241-265 (in Japanese).

5. E. G. Ellison, "A Review of the Interaction of Creep and Fatigue," Journal Mechanical Engineering Science, Vol. 11, No. 3, 1969, pp. 318-339.

6. E. N. da C. Andrade and K. H. Jolliffe, "The Flow of Polycrystalline Metals under Simple Shears," Proceedings of the Royal Society of London, Vol. 213A, 1952, pp. 3-26.

*7. JoDean Morrow and G. R. Halford, "Creep under Repeated Stress Reversals," Joint International Conference on Creep, The Institute of Mechanical Engineers, London, 1963, pp. 3-43 to 3-47.

*8. C. E. Jaske, "The Influence of Temperature on Reversed Creep," MS Thesis, Department of Theoretical and Applied Mechanics, University of Illinois, Urbana, Illinois, 1967. See also T&AM Report No. 674.

*9. Masaki Kitagawa, "Enhanced Grain Boundary Sliding during Reversed Creep of Lead," MS Thesis, Department of Theoretical and Applied Mechanics, University of Illinois, Urbana, Illinois, 1968. See also T&AM Report No. 319.

10. H. Conrad, "Effect of Changes in Slip Direction on the Creep of Magnesium Crystals," Transactions of the Metallurgical Society of AIME, Vol. 215, Feb., 1959, pp. 58-63.

11. A. N. Hughes, "Creep of a 20%Cr/25%Ni/Nb Steel under Reversed Creep Conditions," TRG Report 1018 (6), United Kingdom Atomic Energy Authority, 1965.

12. R. W. Swindeman, "The Interaction of Cyclic and Monotonic Creep Rupture," Joint International Conference on Creep, The Institute of Mechanical Engineers, London, 1963, pp. 3-71 to 3-76.

*13. Masaki Kitagawa, C. E. Jaske, and JoDean Morrow, "Influence of Temperature on Reversed Creep," Fatigue at High Temperature, STP No. 459, American Society for Testing and Materials, 1969, pp. 100-110.

*14. L. B. Freund, "Effect of Repeated Stress Reversals on the Creep of Lead," Fourth Student Symposium on Engineering Mechanics, T&AM Report No. 262, Department of Theoeretical and Applied Mechanics, University of Illinois, Urbana, Illinois, 1964.

15. I. S. Servi and N. J. Grant, "Creep and Stress Rupture Behavior of Aluminum," Transactions of AIME, Journal of Metals, Vol. 191, 1951, pp. 909-916.

16. B. R. Gain and G. M. Sinclair, "Parameter Representation of Dynamic Equilibrium in Creep and Fatigue," Transactions of ASME, Journal of Basic Engineering, Vol. 92, 1970, pp. 610-618.

17. A. P. Boresi, Elasticity in Engineering Mechanics, Prentice-Hall, New Jersey, 1965, p. 87.

18. R. N. Stevens, "Grain Boundary Sliding in Metals," Metallurgical Reviews, Vol. 2, 1966, pp. 129-142.

*19. R. A. Testin, "Investigation of Orthorhombic Grain Size as a Function of Applied Shear Stress in Reversed Creep of Lead," Ninth Student Symposium on Engineering Mechanics, T&AM Report No. 332, Department of Theoretical and Applied Mechanics, University of Illinois, Urbana, Illinois, 1970.

20. K. U. Snowden and J. N. Greenwood, "Rectangular Cracking in Lead," Transactions of the Metallurgical Society of AIME, Vol. 212, February, 1958, pp. 91-92. See also: K. U. Snowden, "The Effect of Atmosphere on the Fatigue of Lead," Acta Metallurgica, Vol. 12, March, 1964, pp. 295-303.

21. S. Takeuchi and T. Homma, "On the Characteristics of Grain Boundary Migration in Pure Metals under the Fatigue at Elevated Temperatures," Transactions of the Japan Institute of Metals, Vol. 7, 1966, pp. 39-46.

22. J. T. Blucher and N. J. Grant, "Low Strain Rate, High Strain Fatigue of Aluminum as a Function of Temperature," Transactions of the Metallurgical Society of AIME, Vol. 239, June, 1967, pp. 805-813.

23. W. Knapp, "The Effects of Specimen Grain Size and Environment on the Fatigue Life of OFHC Copper," UTIAS Technical Note No. 124, Institute for Aerospace Studies, University of Toronto, June, 1968.

24. H. D. Williams and C. W. Corti, "Grain Boundary Migration and Cavitation during Fatigue," Metal Science Journal, Vol. 2, 1968, pp. 28-31.

25. R. L. Stegman and M. R. Achter, "Failure Modes in Nickel Fatigued in Vacuum as a Function of Temperature and Purity," Transactions of Metallurgical Society of AIME, Vol. 239, June, 1967, pp. 742-747.

26. M. J. May and R. W. K. Honeycombe, "The Effect of Temperature on the Fatigue Behavior of Magnesium and Some Magnesium Alloys," Journal of the Institute of Metals, Vol. 92, 1963-1964, pp. 41-49.

27. R. C. Gifkins, A. Gittins, R. L. Bell , and T. G. Langdon, "The Dependence of Grain-Boundary Sliding on Shear Stress," Journal of Materials Science, Vol. 3, 1968, pp. 306-313.

28. Frank Garofalo, Fundamentals of Creep and Creep Rupture in Metals, The Macmillan Company, New York, 1963, pp. 127-146.

29. R. C. Gifkins, "Grain Boundaries and Creep in Metals," The Journal of the Australian Institute of Metals, Vol. 8, No. 2, 1963, pp. 148-157.

*30. Howard Rosenmayer, "The Recrystallization of Lead Subjected to Reversed Creep," Eighth Student Symposium on Engineering Mechanics, T&AM Report No. 681, Department of Theoretical and Applied Mechanics, University of Illinois, Urbana, Illinois, 1969.

31. Manual on Low Cycle Fatigue, STP No. 465, American Society for Testing and Materials, 1969.

32. JoDean Morrow and F. R. Tuler, "Low Cycle Fatigue Evaluation of Inconel 713C and Waspaloy," Transactions of the ASME, Journal of Basic Engineering, Vol. 87, 1965, pp. 275-289.

*33. P. A. Lilienthal, "Description of a Torsion System with Explanatory Data on Accelerated Creep due to Multiple Stress Reversals," MS Thesis, Department of Theoretical and Applied Mechanics, University of Illinois, Urbana, Illinois, 1967.

34. R. L. Bell and T. G. Langdon, "An Investigation of Grain-Boundary Sliding during Creep," Journal of Materials Science, Vol. 2, 1967, pp. 313-323.

Table 1: Summary of Published Work on Reversed Creep

Metal & Ref.	Temp.	No. of Reversals	Type & No. of Tests		Remarks
99.9% Pure Cd (6)	$0.5T_m$	1 or 2	Shear of disk	5	Deceleration
99% Pure Pb (6)	$0.5T_m$	1 or 2	" " "	5	Acceleration
99.9% Pure Pb (6)	$0.5T_m$	1 or 2	" " "	7	Acceleration
Chemical Pb (7)	$0.5T_m$	100	Torsion of tube	13	Acceleration-Creep rate increased about ten times after 60-100 reversals
1100-F Al (8, 13)	$0.32\text{-}0.55T_m$	60	" " "	15	Acceleration at high temperature Deceleration at low temperature
Chemical Pb (9)	$0.5\text{-}0.7T_m$	60	" " "	5	Acceleration
Magnesium (10) single crystal	$0.32T_m$	10	Direct shear on basal plane	1	Deceleration
20%Cr/25%Ni/ Nb steel (11)	$0.55T_m$	> 60	Axial	2	Acceleration
Inconel (12)	$0.65T_m$	1000	"	1	Acceleration
Chemical Pb (14)	$0.5T_m$	20	Torsion of tube	8	Acceleration-The steady creep rate after stress reversals was much larger than that of virgin lead.

Table 2: Heat Treatment Conditions

1100-F aluminum	Annealed at 620 K for half hour in vacuum, cooled in vacuum furnace
Chemical lead	Annealed at 373 K for one hour in boiling water, cooled in air
OFHC copper	Annealed at 873 K for one hour in vacuum, cooled in vacuum furnace

Table 3: Summary of Published Work on Grain Boundary Migration during Cyclic Deformation

Metal & Purity	Ref.	Type of Test	Temp.	Formation of the Orthorhombic Grains
FCC				
Pb - 99.9%	9	Torsional reversed creep	$0.5\text{-}0.7\,T_m$	yes
99.99%	20,21	Torsional & axial fatigue	$0.5\,T_m$	yes
Al - 99%	--	Torsional reversed creep	$0.3\text{-}0.55\,T_m$	no
99.99%	21,22	Torsional & axial fatigue	$0.69\text{-}0.81\,T_m$	yes
99.999%	21	Torsional & axial fatigue	$0.83\,T_m$	yes
Cu - 99.96%	23	Torsional fatigue	$0.46\,T_m$	yes
99.99%	--	Torsional reversed creep	$0.6\,T_m$	yes
Vacuum melted	24	Torsional & axial fatigue	$0.5\,T_m$	yes
Ni - 99.8%	25	Axial fatigue	$0.48\,T_m$	no
99.99%	25	Axial fatigue	$0.48\,T_m$	yes
HCP				
Mg - 99.95%	26	Torsional & axial fatigue	$0.33\text{-}0.57\,T_m$	no
99.98%	24	Torsional & axial fatigue	$0.73\,T_m$	no

APPENDIX A

TORSIONAL REVERSED CREEP TEST APPARATUS

A hydraulic torsional creep testing machine was developed through this program. Motion of a hydraulic rotary actuator was controlled automatically by an electronic servo-controller through a servo-valve. Information on similar mechanical test systems with applications to axial low cycle fatigue tests may be found in Ref. (31). In this section features of our application to the torsional reversed creep tests are described.

Specimens

Two types of tubular specimens, shown in Fig. A1, have been used during this program. For the design of tubular specimens, two considerations are essential; namely, stress distribution across the thickness of the tube and local buckling. The more uniform stress distribution can be obtained the thinner the tube. This increases the possibility of buckling. Compromising these factors, the ratio of outside diameter to wall thickness was taken as about ten. Practical consideration was also given to material bar stock availability, machining and elevated temperature equipment size.

Loading Fixture

The specimen is threaded into a tapered split collet which is then squeezed into a conical hole on the top of the actuator shaft. One of the designs employed for this type of gripping is illustrated in Fig. A2.

This type of gripping was preferred over grips which employ keys and keyways for the following reasons:

1. Good concentricity can be obtained repeatedly for each specimen setup without excessive care or adjustment.

2. Gripping force is distributed uniformly around the circumferential surface.

3. Loosening of key contact due to small clearance and due to the possible plastic deformation on the contact surface may result in backlash which, in turn, causes poor performance under closed loop control.

The torque capacity of this grip is determined by the magnitude of the circumferential friction force and the radius of the contact surface. The employed dimensions were satisfactory for most of the test program. However, when a larger torque is applied (for example, torsional tests of hard steel), the ratio of thread diameter to test section diameter must be increased.

Creep deformation under the gripping force is sometimes a problem at high temperature. This leads to a gradual reduction of the friction force and slip at the thread. During the earlier phase of the experimental program, slip at the thread was encountered in some tests under high torque. The addition of two thick-walled tubes inside of the threaded end portions of the specimens prevented this problem thereafter.

The upper end of specimen type A was simply inserted into a conical hole in the upper grip and clamped by two sets of bolts and locknuts. For specimen type B, the same mechanism as that of the lower grip was employed.

The upper grip is connected to the load frame through a torque cell and a splined shaft frozen in a Wood's metal grip (29). Wood's metal in the grip was easily melted and solidified in several minutes by allowing steam or cold water to flow through channels drilled through the splined shaft.

Specimen setup procedure is as follows:

1. Tighten the upper grip.
2. Melt the Wood's metal, and then tighten the lower grip.
3. Solidify the Wood's metal after setting the crosshead to the proper height.

The use of the Wood's metal grip with this procedure minimizes clamping distortions. To allow axial freedom to accommodate the specimen length change during heating, a splined shaft or a similar mechanism was also inserted between the upper grip and the Wood's metal pot.

Rotary Actuator and Journal Bearing

Rotary motion is supplied by a hydraulic rotary actuator with a maximum torque capacity of 4000 in. -lb. and a rotation of 280 degrees.

After trying several ways of assuring the concentricity of rotary motion, a cast-in-place journal bearing was found to give the best results. The journal bearing was built by the following procedure:

1. A layer of teflon tape was first wound around the shaft.
2. A rigid holder was tightened to the load frame table around the shaft.
3. Wood's metal was cast in the space between the holder and actuator shaft.

This teflon tape reduces the friction to the extent that smooth rotary motion is possible. With this journal bearing, eccentricity of rotary motion was reduced to less than 0.0015 inches.

Measurement of Test Variables

Torque was measured by a strain-gaged cell of 200 in. -lb. capacity which was placed in series with the specimen. The signal from the torque cell was fed into the servo-controller as a feedback signal.

For the measurement of the angle of twist between the shoulders of the specimen, a rotary variable differential transformer (RVDT) or a strain-gaged linear clip gage was used. Both of these devices are commercially available and have good sensitivity and dependability. Several attachments were designed and used to transmit the angle of twist to the RVDT or clip gage. Since the RVDT itself is fairly heavy, the attachments tend to be heavier and/or clamping force to the specimen tends to be larger than those for the clip gage, unless the RVDT is supported in some way.

Two types of devices designed for use with the RVDT were described in detail by Lilienthal (33) and Jaske (8). In the former, devices are clamped outside of the specimen gage length and the angle of twist is first converted to the relative motion of two coaxial cylinders and then to the RVDT. In the latter, two concentric probes were fastened inside the specimen, and the other ends of the probes were directly connected to the case and shaft of the RVDT.

A recently employed method using a strain-gaged linear clip gage is shown in Fig. A3. Two collars are clamped onto the shoulders of the specimen. A small rod is attached on each collar in the direction parallel to the specimen axis. Each rod is inserted into a hole in a small teflon block which is connected to each arm of the clip gage. This device is simpler, more compact and naturally lighter than the two devices mentioned above. Although this device measures the sine of the angle of twist, it is possible to measure an angle of twist of $\pm$ 10 degrees within 0.2% linearity or $\pm$ 20 degrees within 1% linearity.

Heating the Specimen and Temperature Measurement

Specimens were heated by one of two apparatus; a commercially available three-zone radiant heater of 3 kW capacity which surrounds the reduced section of the specimen, or by an internal resistance heating element located inside of the tubular specimen. The heating element is made of a stainless steel rod which has two reduced sections, as shown in Fig. A4, and powered by a 30 kVA welding transformer.

The dimension of the reduced section of the heating rod can be adjusted for uniform temperature distribution. The internal heating element has the advantage that the outside of the specimen is kept free for observations during the tests. Using these devices, the temperature along the specimen gage length was controlled within $\pm$ 5 C. The maximum operable temperature was about 500 C for both devices.

The temperature was measured on the outside surface of the specimen using three chromel-alumel thermocouples fastened by glass fiber tape. Temperature, torque and angle of twist were recorded on strip chart recorders.

Control for Reversed Creep Tests

Reversed creep tests require continuous control of stress as well as control of the strain limit, as is shown in Fig. 1 of the main text. While both the stress amplitude and strain range are kept constant throughout a test, the strain rate changes depending on the changes in material deformation resistance. The usual servo-control was modified for this type of test in the following manner:

1. The stress signal is fed back to the servo-controller as a primary feedback signal and the shear stress is controlled continuously.
2. Simultaneously the strain signal is fed into the command signal generator which consists of a flip-flop circuit and a strain limiter. When the strain signal reaches the preset limits, the position of the flip-flop circuit is altered by a triggering signal from the limiter. The function generator produces a square wave whose frequency alters from cycle to cycle depending on the changes in the material deformation resistance. The output of this function generator is used as the command signal to the servo-controller.

APPENDIX B

ACCELERATION OF CREEP CAUSED BY GRAIN BOUNDARY REORIENTATION

by

Masaki Kitagawa

Based on the observations of Gifkins et al. (27), it is assumed that the amount of sliding during a certain period of time is approximated by the following power function of the resolved shear stress, τ_{rss}, on each grain boundary;

$$U_{gb} = A\tau_{rss}^{m} \tag{B1}$$

where A and m are material constants. Using this approximation a component of grain boundary sliding in the circumferential direction under an applied shear stress, τ_a, can be calculated as

$$U_{gb}(\theta, \Psi) = \frac{A\tau_a^{m} \left[(1-\cot^2\theta)^2 + (1+\cot^2\theta)\cot^2\Psi\right]^{\frac{m-1}{2}} (1-\cot^2\theta + \cot^2\Psi)}{(1+\cot^2\theta + \cot^2\Psi)^{m+\frac{1}{2}}} \tag{B2}$$

for a grain boundary oriented in the direction illustrated in Fig. B1. This equation can be derived by 1) calculating the maximum shear vector on the grain boundary of the given orientation (θ, Ψ), 2) raising the magnitude of the maximum shear stress by m'th power, and finally, 3) converting this vector into the circumferential direction.

Bell and Langdon (34) measured the distribution of the angle Ψ in a longitudinal cross section and found that the probability of the occurrence of the boundaries making an angle Ψ with the specimen surface was proportional to $\sin(\Psi)$. Since in a random grain structure this distribution should not depend on the orientation of the cross section, the probability of occurrence of a longitudinal line on the surface to cross the grain boundaries of an orientation θ would be also proportional to $\sin(\theta)$. Therefore, for the boundaries of a given orientation (θ, Ψ), the probability of crossing the longitudinal line may be approximated by

$$(\text{constant})\ \sin(\Psi)\ \sin(\theta) \tag{B3}$$

An average of the grain boundary sliding, $\overline{U}_{gb}$, in a random grain structure can be calculated by taking an arithmetic mean of $U_{gb}(\theta, \Psi)$ weighted by this probability; i.e.,

$$\overline{U}_{gb} = \frac{\iint U_{gb}(\theta, \Psi) \sin\Psi \sin\theta \, d\theta \, d\Psi}{\iint \sin\Psi \sin\theta \, d\theta \, d\Psi} \tag{B4}$$

or

$$\overline{U}_{gb} = \frac{1}{\beta} A \tau_a^m \tag{B5}$$

where β is an averaging factor which accounts for the distribution of grain boundary orientation. The calculated values of β are listed in Table B1 for various stress dependence exponents, m. A similar calculation is done for the grain boundary sliding in the longitudinal direction, and β's are the same as above.

In the orthorhombic grain structure, the θ is everywhere zero or 90 degrees and Ψ is everywhere 90 degrees. Then β will be one for the orthorhombic grain structure.

If one assumes that there is no change in grain size, then shear strain due to grain boundary sliding, γ_{gb}, would increase by a factor of β when all grain boundaries are reoriented onto the maximum shear planes; i.e.

$$\gamma_{gb}^r = \beta \, \gamma_{gb}^o \tag{B6}$$

where superscripts o and r indicate before and after the reorientation, respectively. In order to separately evaluate the effect of reorientation of grain boundaries, it is further assumed that the creep strain in the grain per unit time does not change; i.e.

$$\gamma_g^r = \gamma_g^o \tag{B7}$$

Then, the over-all creep strain, γ_t, in the orthorhombic grain structure during the same period is

$$\gamma_t^r = \gamma_g^r + \gamma_{gb}^r = \gamma_g^o + \beta \gamma_{gb}^o \tag{B8}$$

Using a parameter, $\alpha = \gamma_{gb}/\gamma_t$, this equation is rewritten as follows:

$$\gamma_t^r = \left[(1-\alpha^o) + \alpha^o \beta\right] \gamma_t^o \tag{B9}$$

or

$$\alpha^r = \frac{\gamma_{gb}^r}{\gamma_t^r} = \beta\alpha^o/(1-\alpha^o + \beta\alpha^o) \tag{B10}$$

These relations are illustrated in Fig. B2. The figure indicates the following:

1. The gradual formation of an orthorhombic grain structure could cause a significant acceleration of creep by increasing the contribution of grain boundary sliding to the over-all creep strain.
2. The magnitude of the effect of the reorientation of grain boundaries on the acceleration of creep depends on both the stress dependence exponent, m, and the strain ratio, α. The larger the values of m and α, the larger the acceleration of creep.
3. However, the observed acceleration of creep (see Fig. 3) is often larger than one calculated here, implying that there are additional factors responsible for the acceleration of creep.

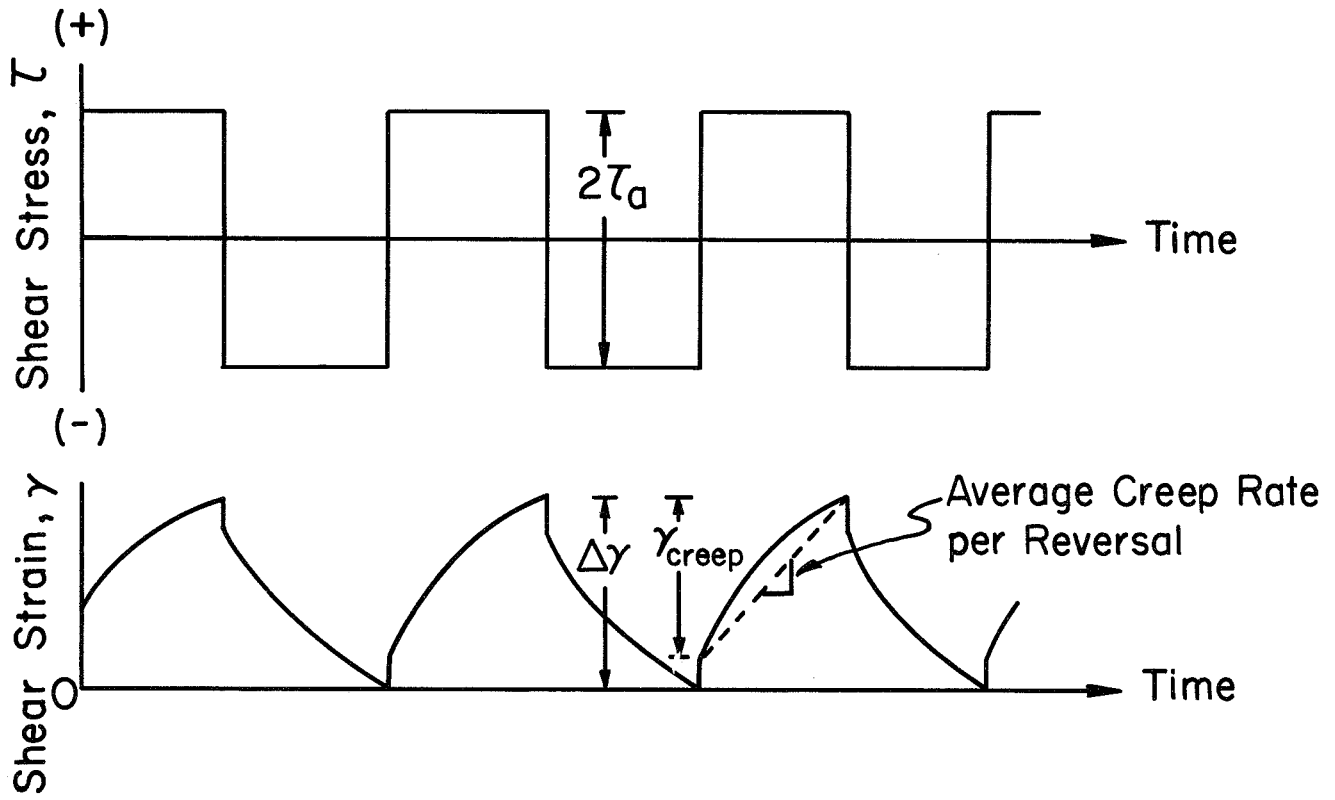

Fig. 1a Schematic Stress-Time and Strain-Time Curves

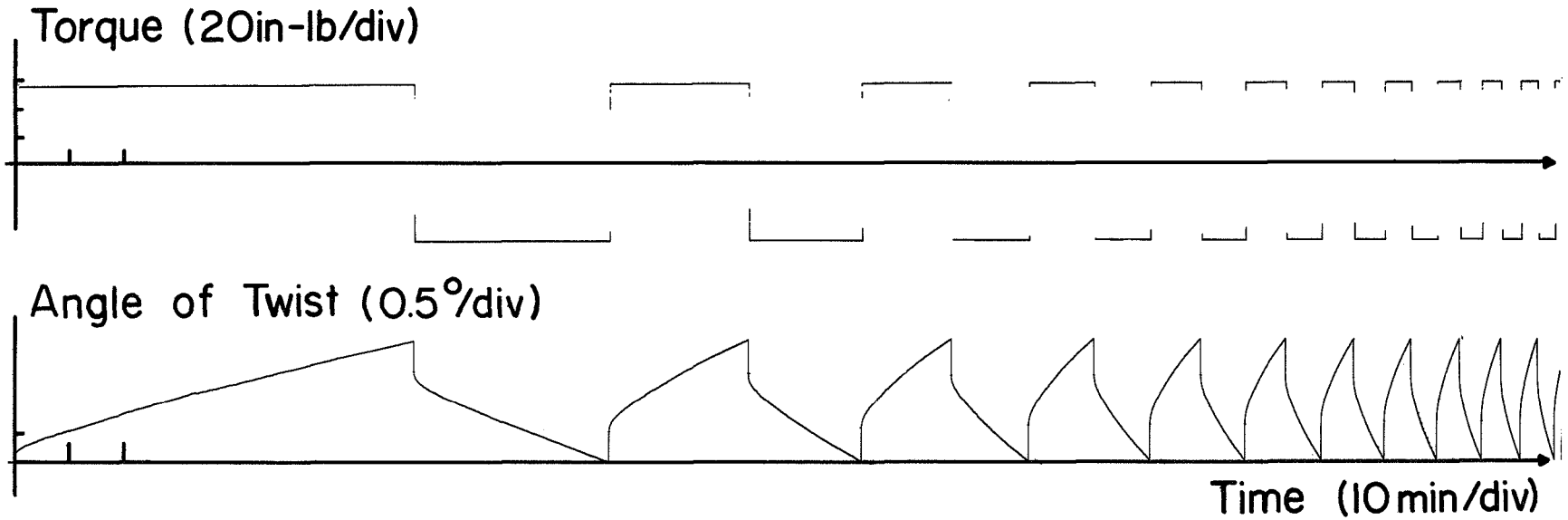

Fig. 1b A Typical Test Record during Acceleration of Creep
(Lead; $T = 0.5\, T_m$, $\tau_a = \pm 600$ psi, $\Delta\gamma = 0.0173$)

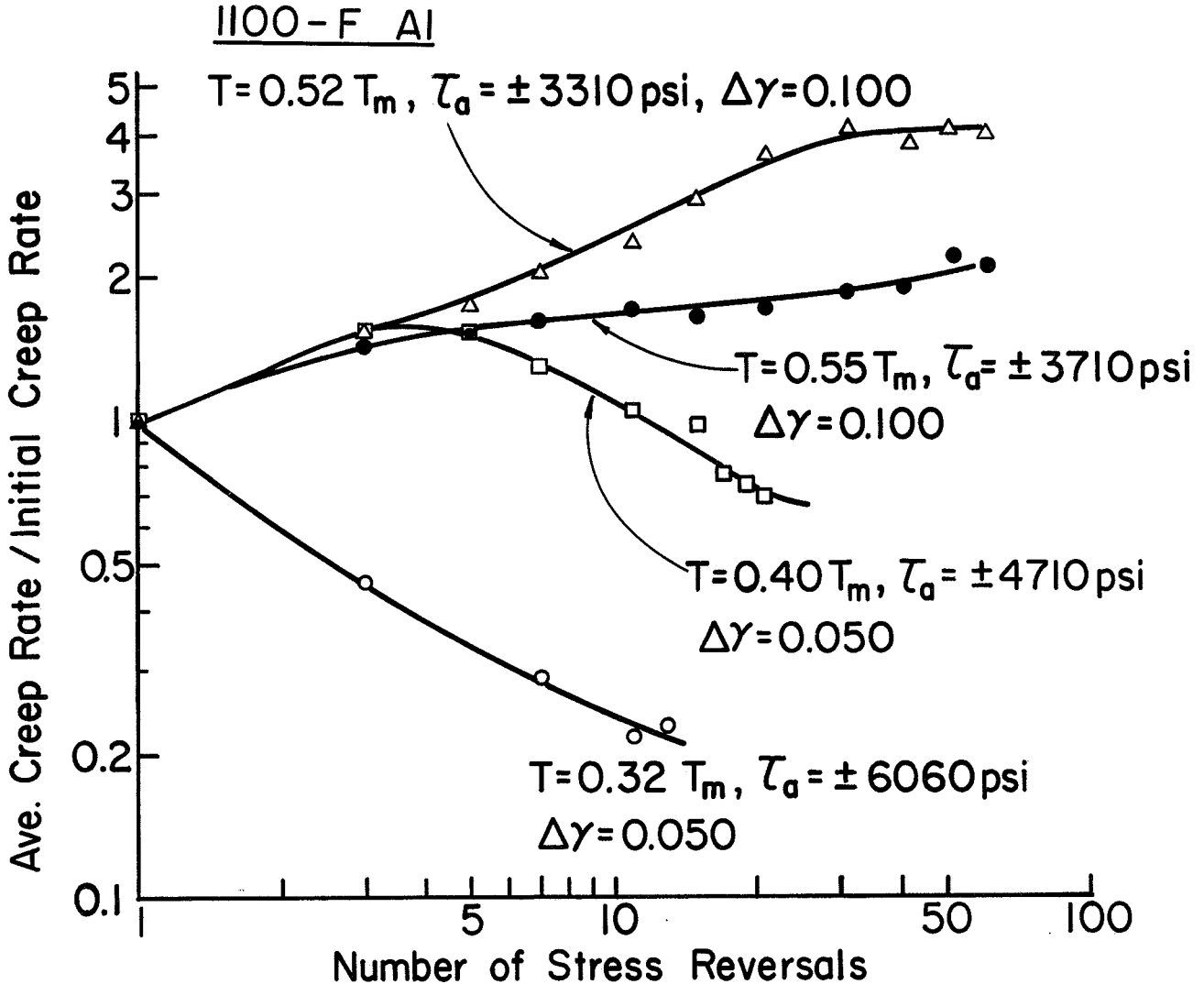

Fig. 2a Change in Average Creep Rate with the Number of Stress Reversals (Ref. 13)

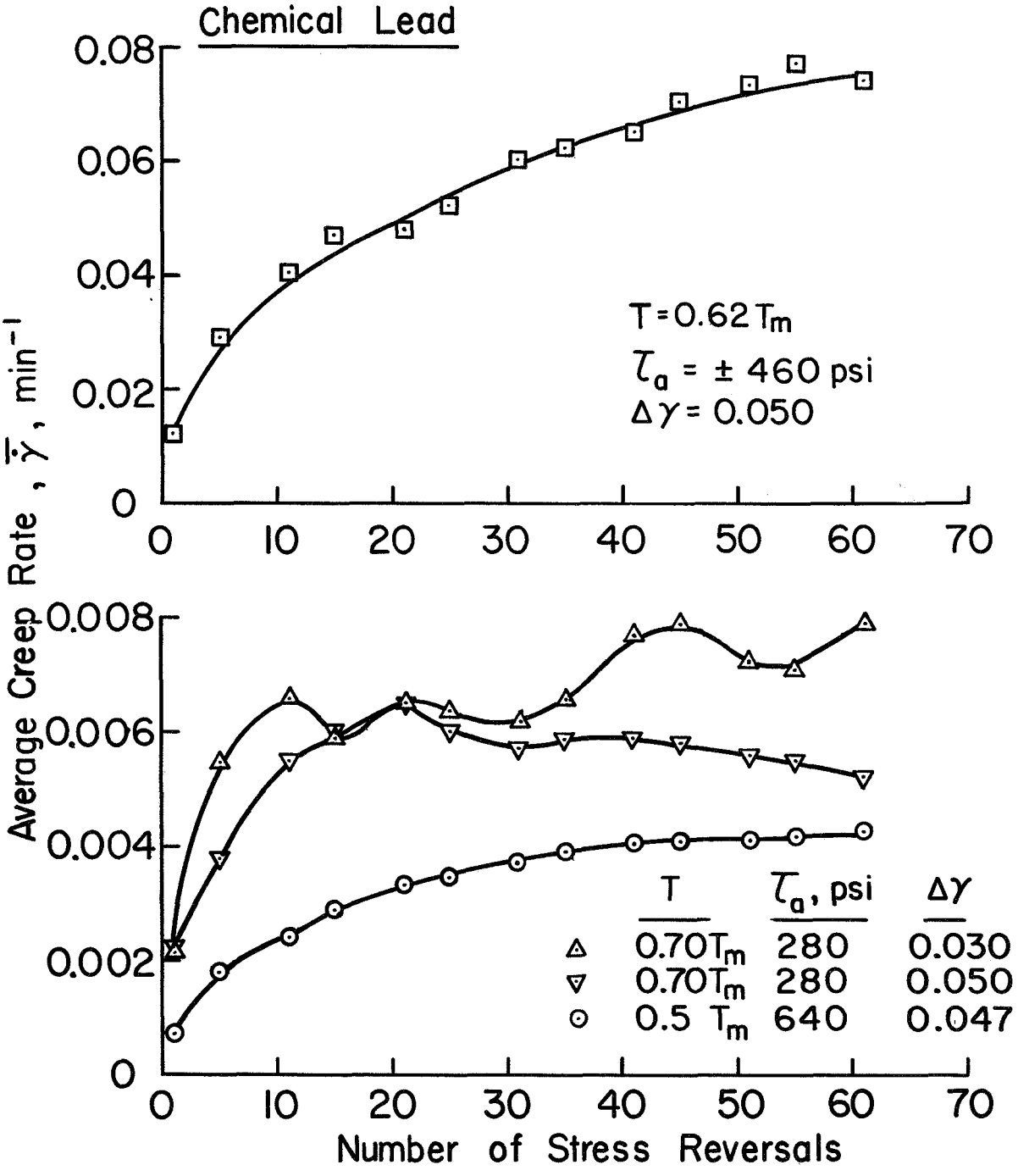

Fig. 2b The Change in Average Creep Rate of Lead at Various Temperatures (Ref. 9)

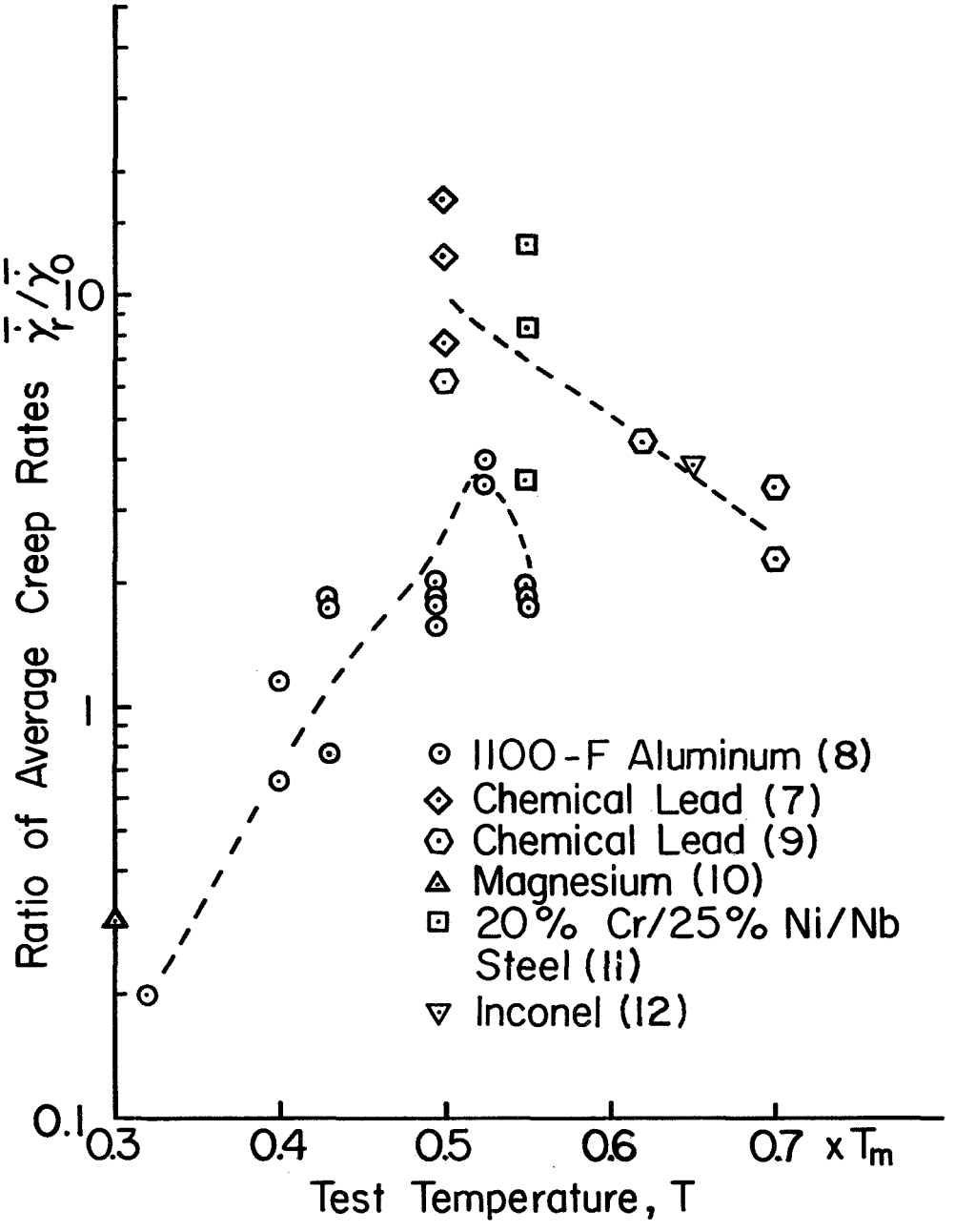

Fig. 3 Change in Average Creep Rate after Multiple Stress Reversals as a Function of Temperature

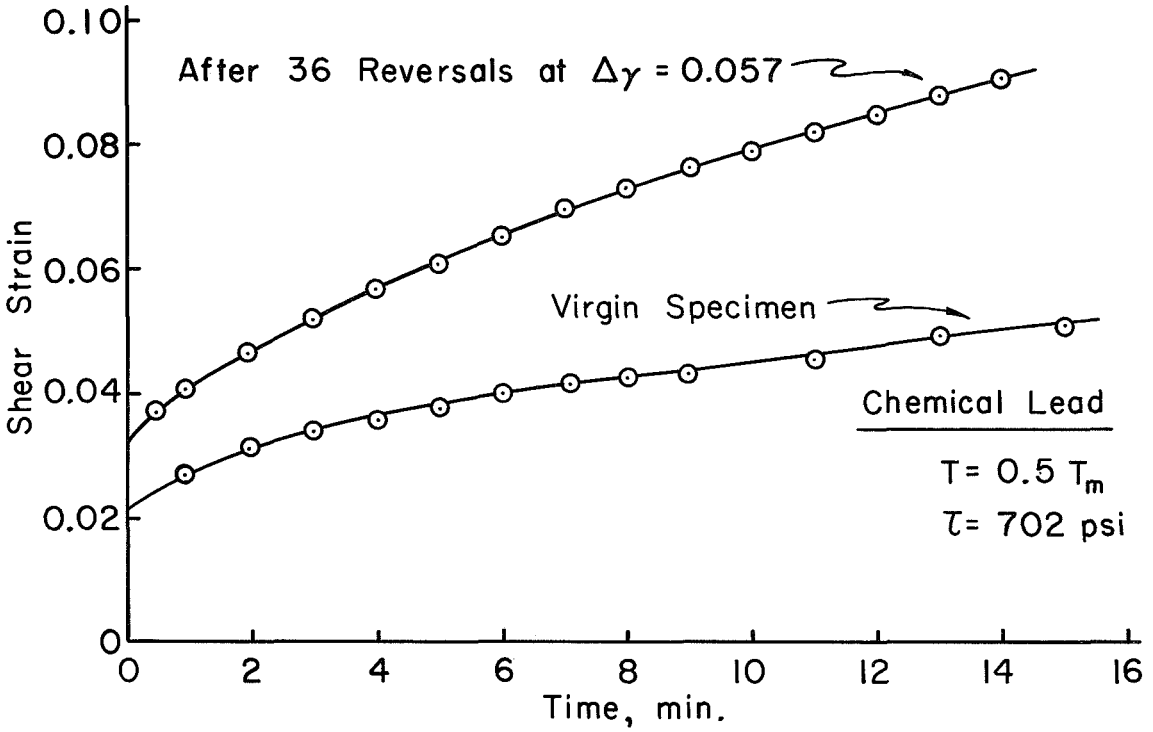

Fig. 4 Effect of Multiple Reversals on Static Creep Curve (Ref. 14)

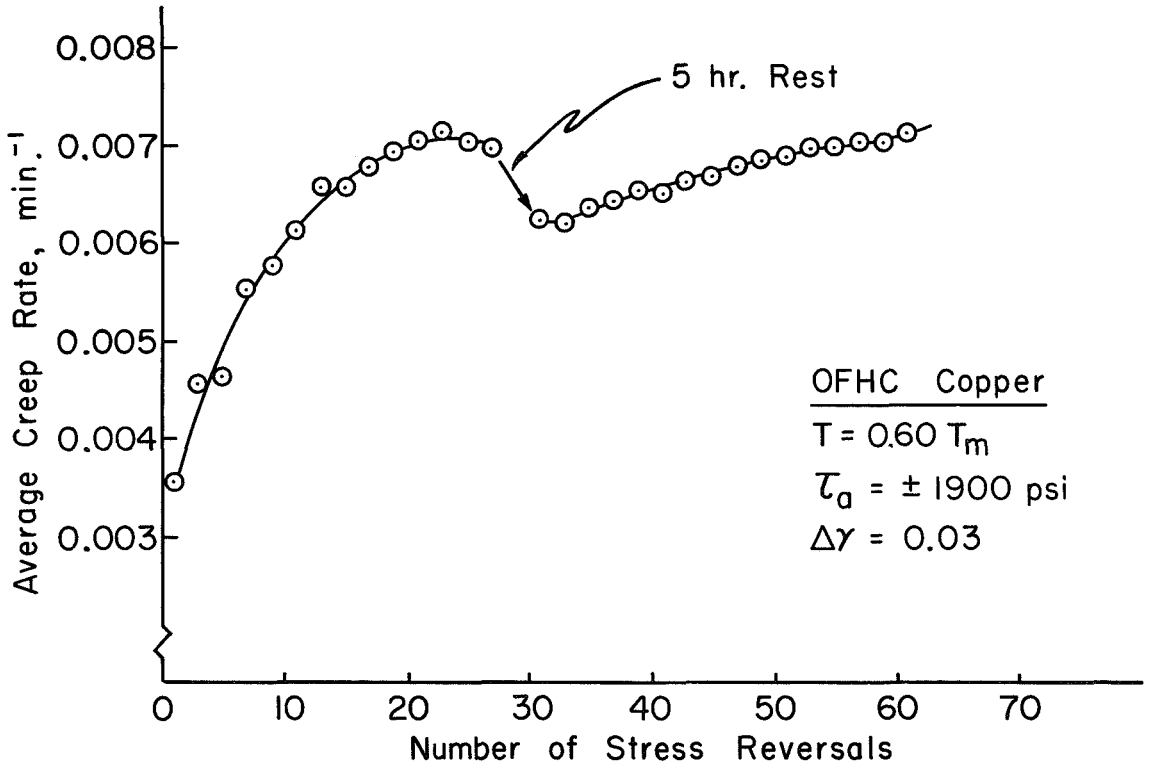

Fig. 5 Influence of Rest Period on Average Creep Rate

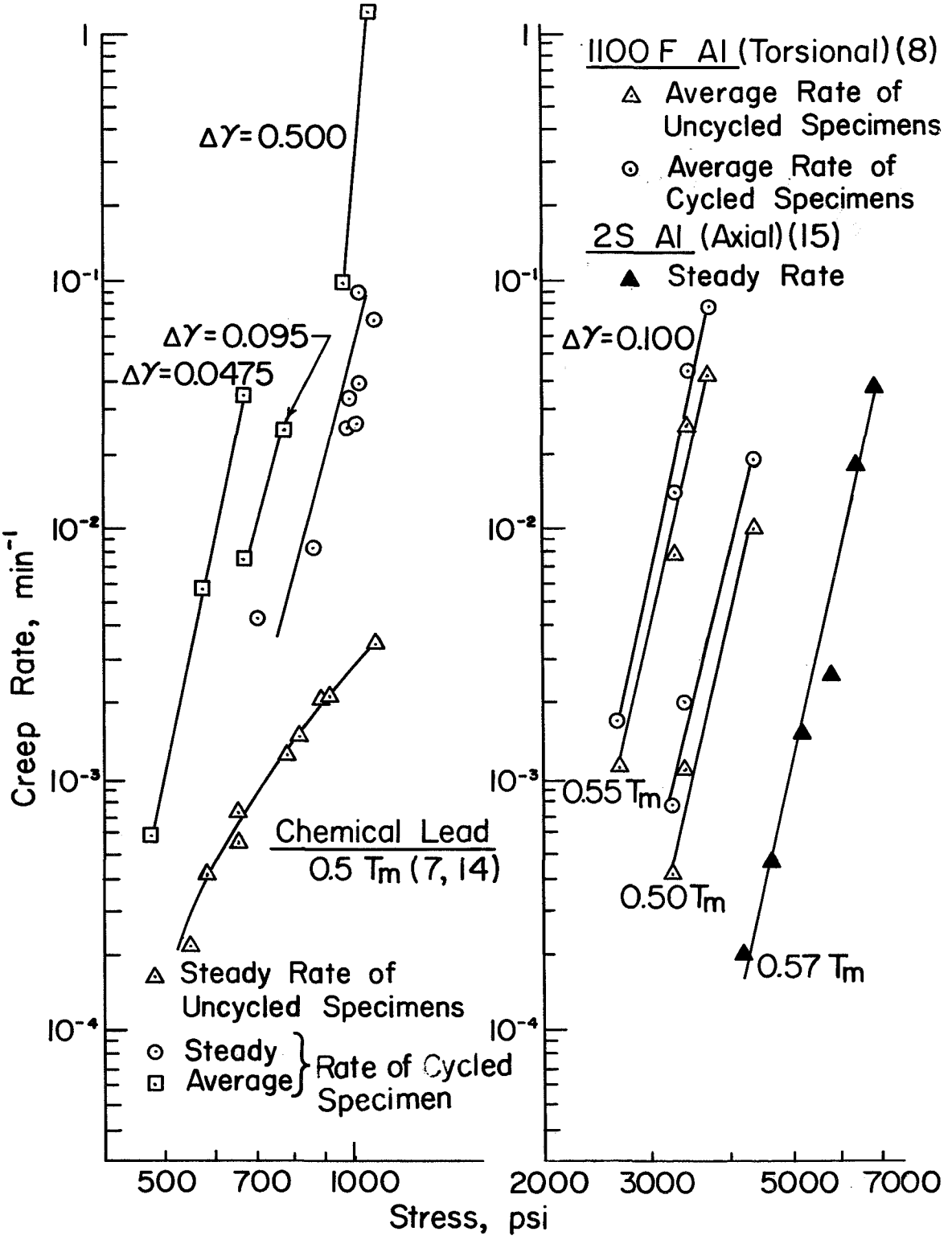

Fig. 6 Comparison of Stress Dependence

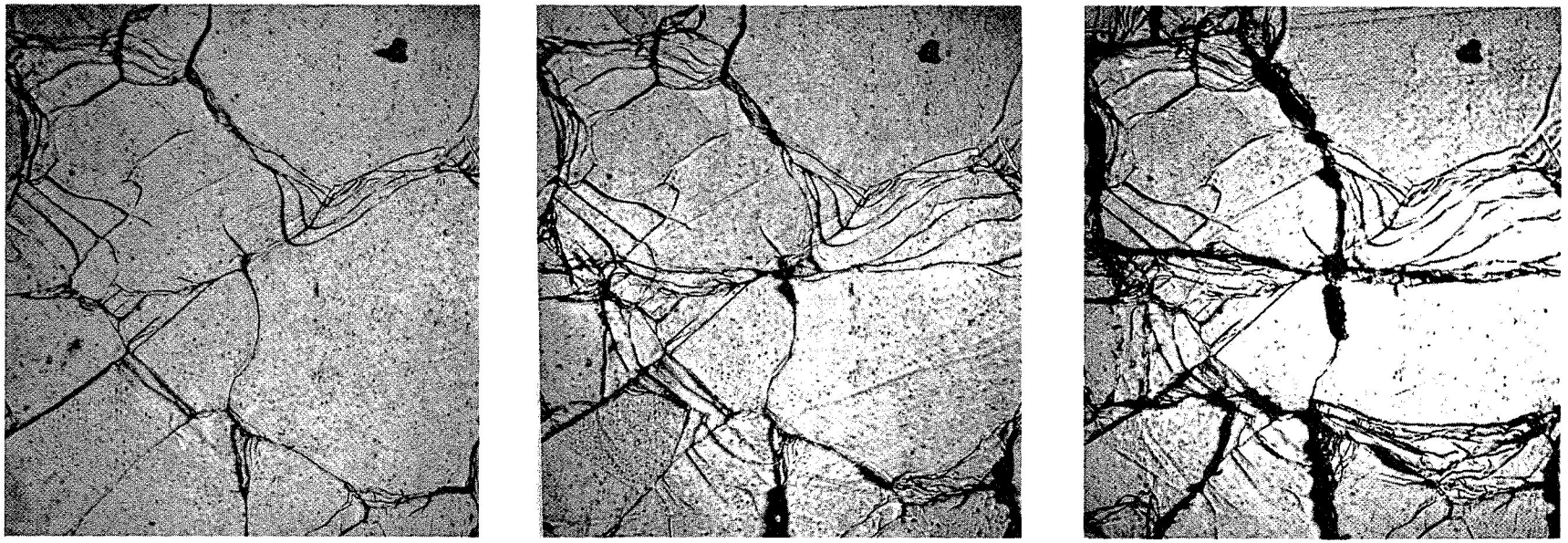

Fig. 7 Grain Boundary Migration toward the Maximum Shear Planes during Reversed Creep of Lead ($\tau_a = \pm 550$ psi, $\Delta\gamma = 0.03$, $T = 0.5\, T_m$)

(b) Transverse Cross Section

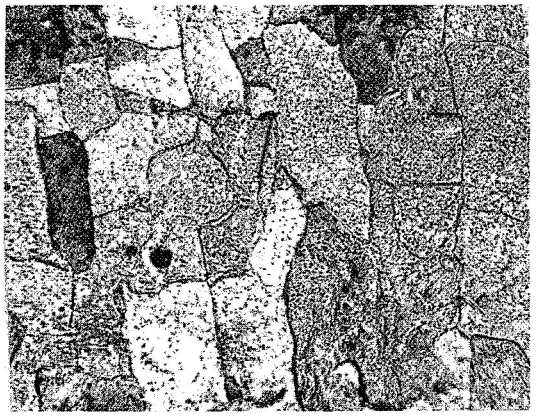

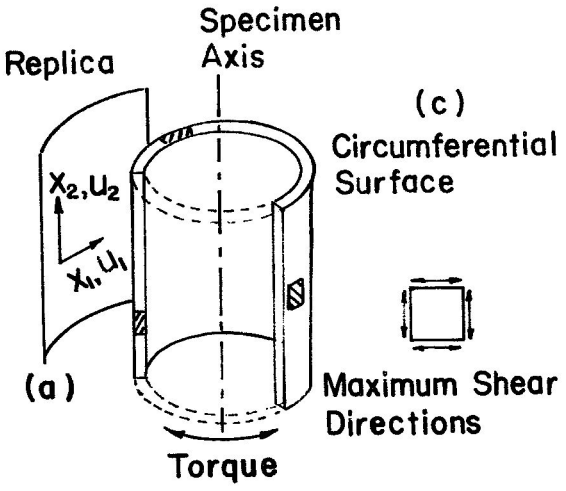

(d) Longitudinal Cross Section

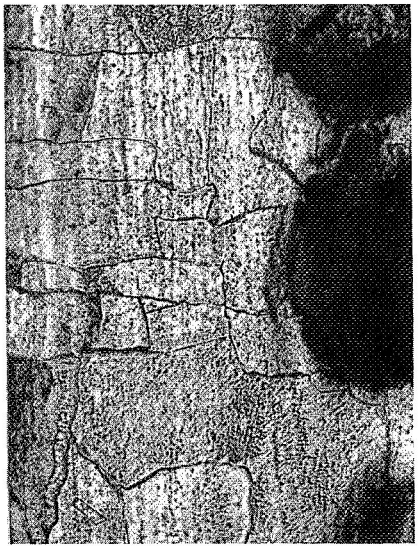

Fig. 8 Cross Sections and Surface of a Lead Specimen after Reversed Creep ($T=0.5T_m$, $\tau_a=\pm 640$psi, $\Delta\gamma=0.047$) Showing that Grain Shape is Orthorhombic. (Ref. 9)

0.2 mm

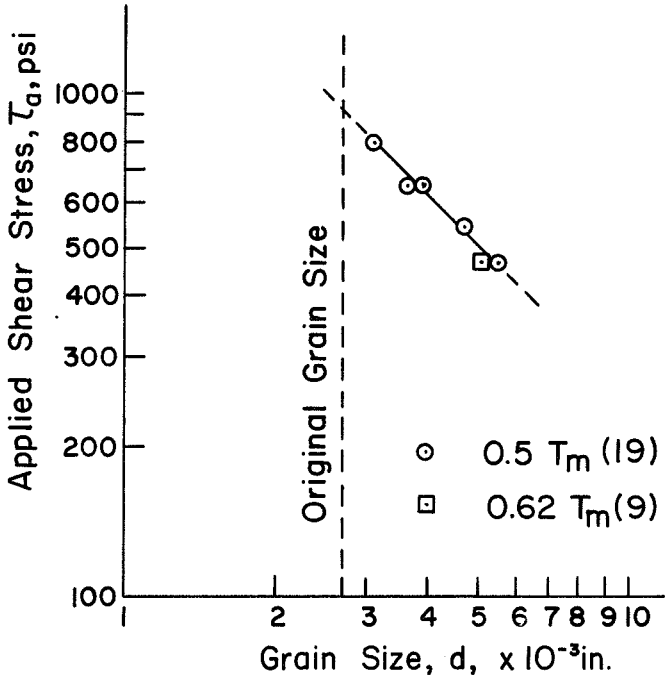

Fig. 9 Applied Shear Stress vs. Grain Size for Reversed Creep of Lead at Room Temperature, after 78 Reversals

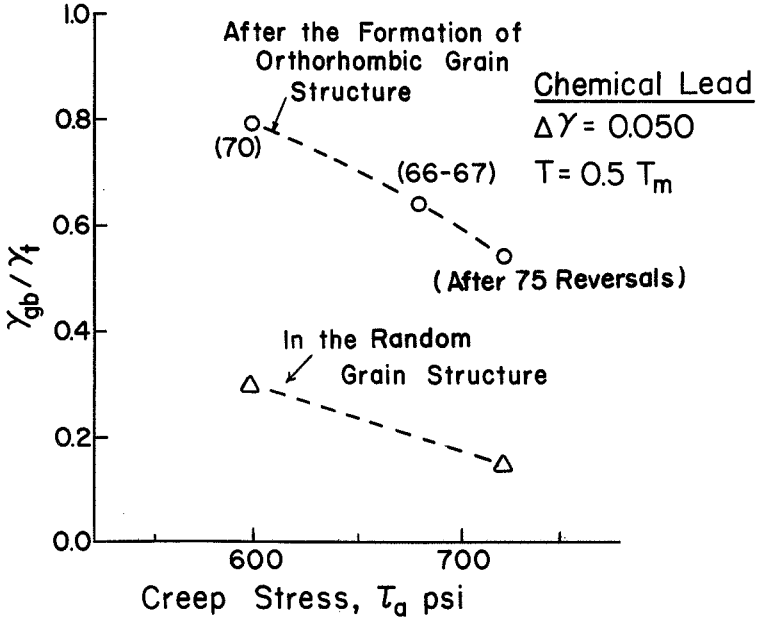

Fig. 10 Comparison of Grain Boundary Sliding Strain in Two Types of Grain Structure

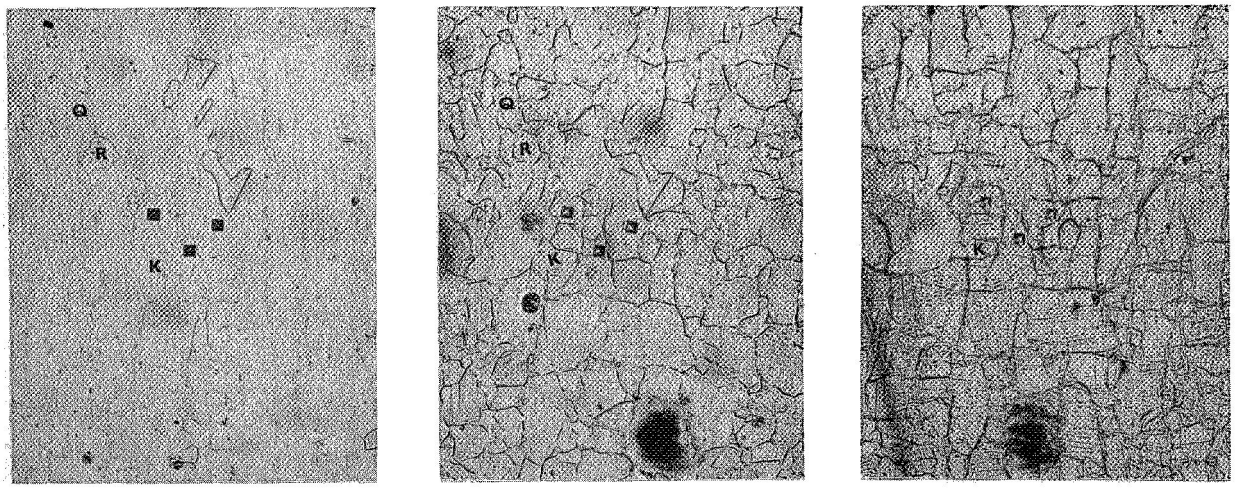

(a) Before Test (b) First Reversal (c) 15th Reversal

(d) 28th Reversal (e) 40th Reversal (f) 67th Reversal

0.5mm

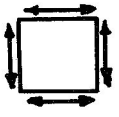

Maximum Shear Direction

Fig. 11 Periodic Observation of Grain Structure during Reversed Creep of Lead; $T=0.5T_m$ $\tau_a = \pm 680$ psi, $\Delta\gamma = 0.050$ (Ref. 9)

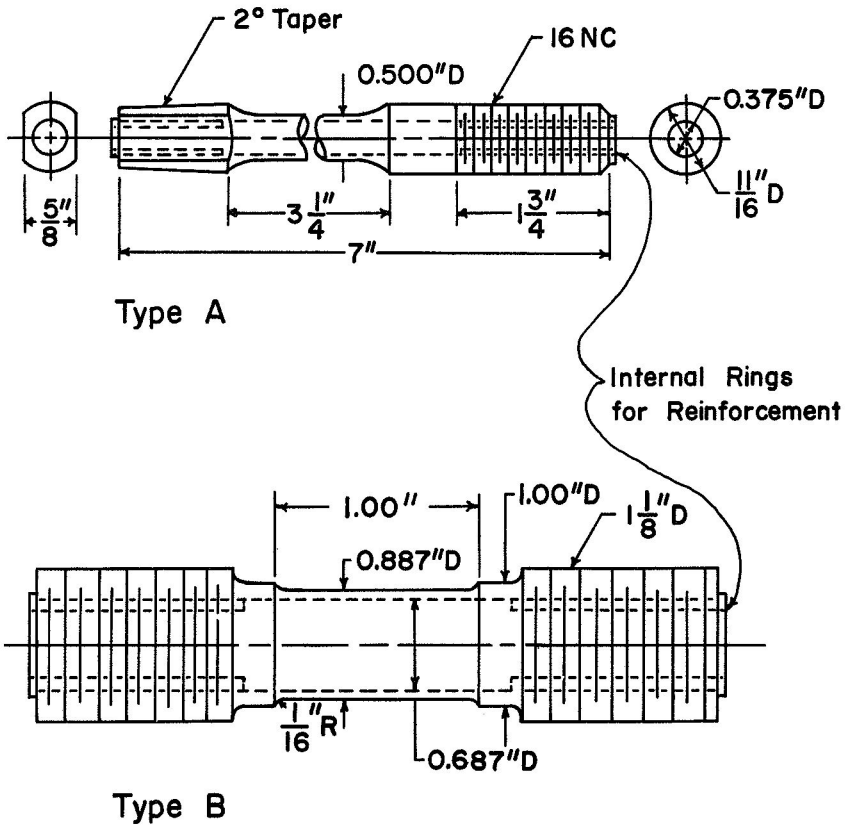

Fig. A1 Specimen Dimensions

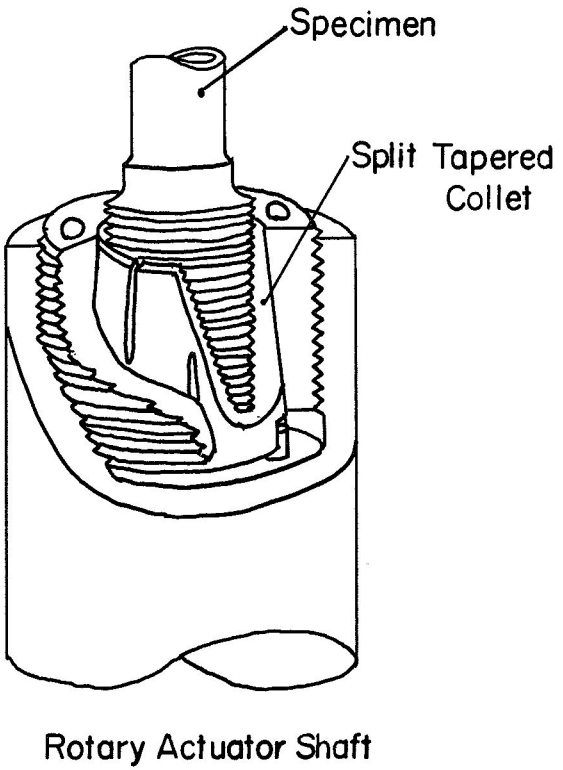

Fig. A2 Torsional Specimen Grip Using a Split Tapered Collet

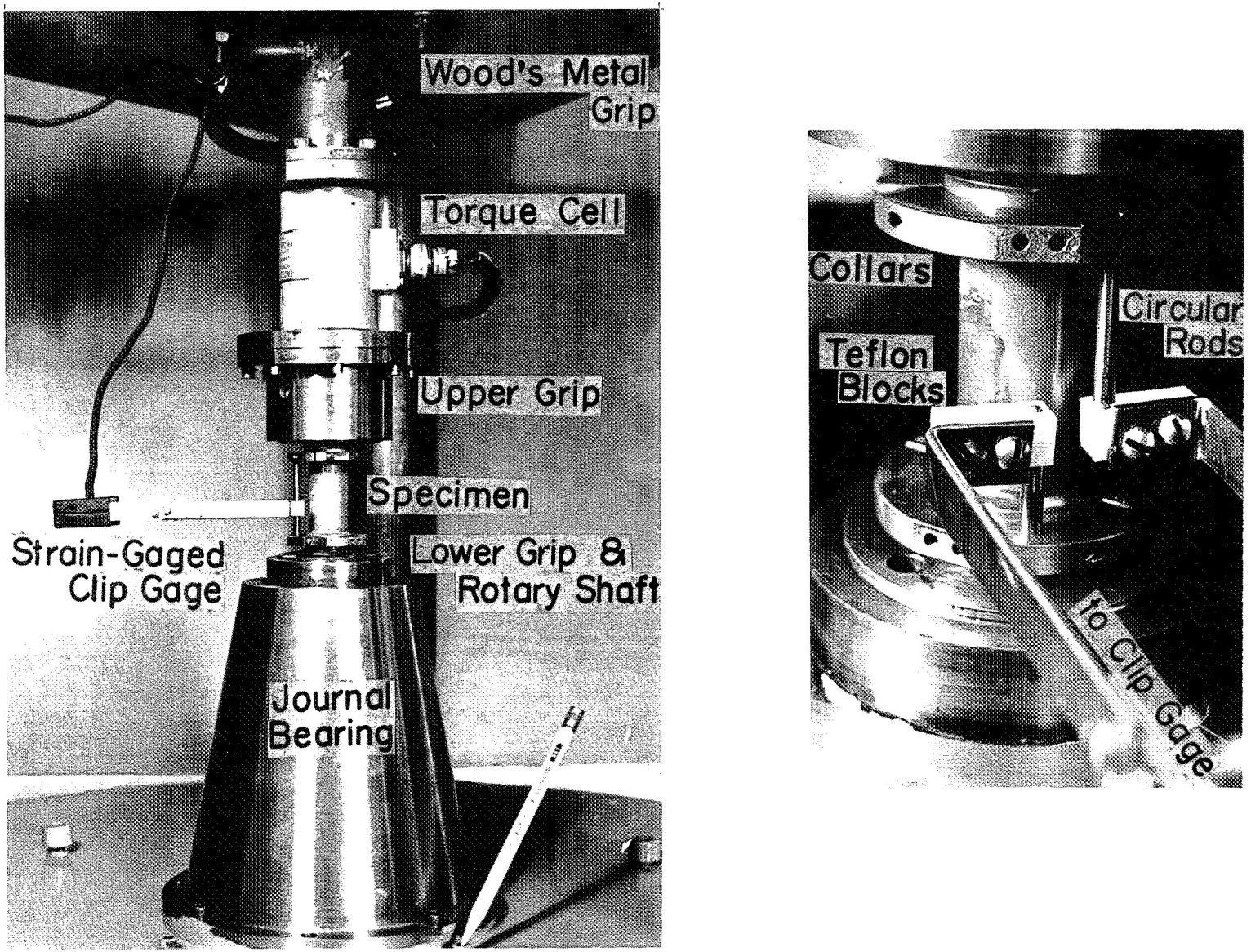

Fig. A3 Setup for Tests at Room Temperature and a Close-up View of Angle-of-Twist Measuring Device

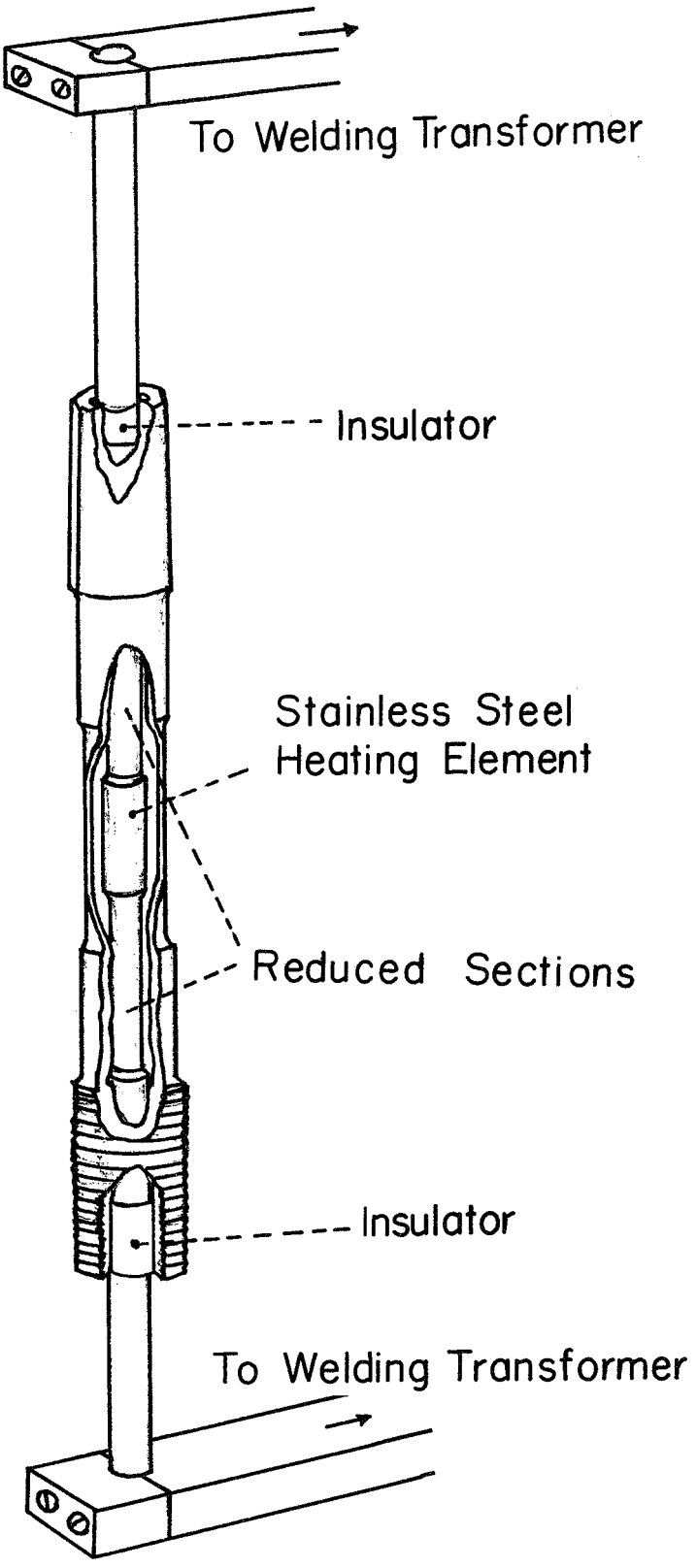

Fig. A4 Internal Resistance Heating

Table B1 Averaging Factor β in Equation B5

m	β
1	3.1
3	5.6
5	7.7
7	10.4
9	13.0

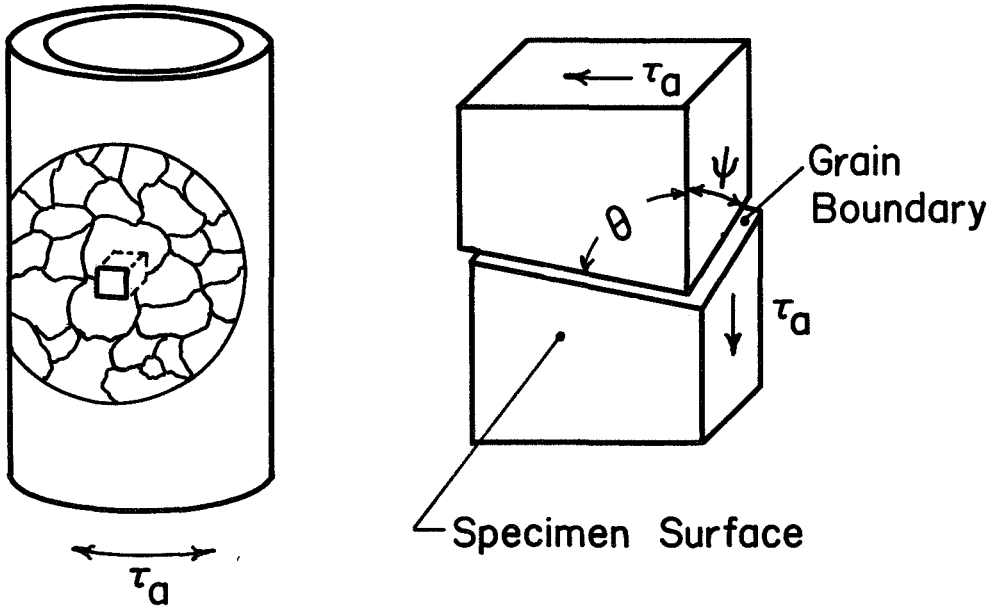

Fig. B1 Grain Boundary Geometry

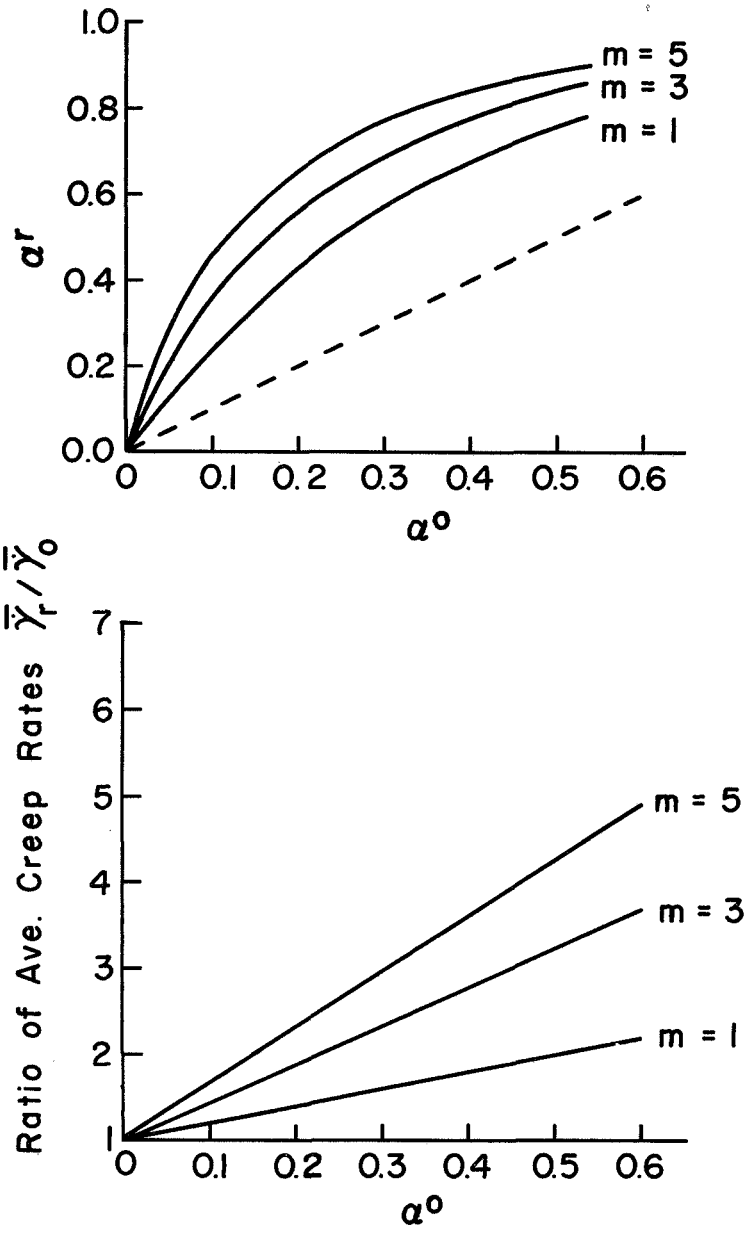

Fig. B2 Expected Changes in Grain Boundary Contribution to Over-all Strain(α) and in Over-all Creep Rate Caused by Reorientation of Grain Boundaries